

Article

Spatial Distribution and Sources of Polycyclic Aromatic Hydrocarbons in Sediments from Dachan Bay, Shenzhen City

Wenjing Huang ¹ , Beibei Liu ¹, Hui Zhao ^{1,2,3,4,*}, Lirong Zhao ^{1,*} and Jibiao Zhang ¹ ¹ College of Chemistry and Environmental Science, Guangdong Ocean University, Zhanjiang 524088, China² Cooperative Research Center for Offshore Marine Environmental Change, Guangdong Ocean University, Zhanjiang 524088, China³ Southern Marine Science and Engineering Guangdong Laboratory, Zhuhai 519082, China⁴ Research Center for Coastal Environmental Protection and Ecological Resilience, Guangdong Ocean University, Zhanjiang 524088, China

* Correspondence: huizhao1978@163.com (H.Z.); zlrms@163.com (L.Z.)

Abstract: The study investigated the composition and content of Σ_{15} PAH in the surface and core sediments from Dachan Bay (DCB) in Shenzhen city and discussed the effects of urban development and regional energy structure on the marine environment through the spatial distribution, vertical profile, and sources of Σ_{15} PAH. The results indicated that the concentrations of Σ_{15} PAH in the sediments of DCB ranged between 299 ng/g and 2336 ng/g in the surface sediments and between 65 ng/g and 994 ng/g in the core sediments. The horizontal spatial distribution of PAHs content with decreasing concentrations from the coastal to central areas implied the land-based input of PAHs. The vertical profile of high PAHs concentration in 0 cm–60 cm suggested that the PAHs pollution is attributed to the urban development of Shenzhen since 1950, especially after the 1980s. According to features of the low molecular weight (LMW)/high molecular weight (HMW), PAHs diagnostic ratios and their relationships with total organic carbon (TOC) and oil, the pyrogenic PAHs were mainly from the combustion of petroleum and byproducts in the surface and 0 cm–60 cm sediments but from the combustion of biomass in 60 cm–190 cm sediments, which corresponded with the variation of energy structure in surrounding areas. This study suggested that urban development and regional energy structure have a great impact on PAHs distribution in DCB and further controls of land-based pollutant emissions are still needed.



check for updates

Citation: Huang, W.; Liu, B.; Zhao, H.; Zhao, L.; Zhang, J. Spatial Distribution and Sources of Polycyclic Aromatic Hydrocarbons in Sediments from Dachan Bay, Shenzhen City. *Water* **2023**, *15*, 1848. <https://doi.org/10.3390/w15101848>

Academic Editor: Chin H Wu

Received: 31 March 2023

Revised: 4 May 2023

Accepted: 9 May 2023

Published: 12 May 2023



Copyright: © 2023 by the authors. Licensee MDPI, Basel, Switzerland. This article is an open access article distributed under the terms and conditions of the Creative Commons Attribution (CC BY) license (<https://creativecommons.org/licenses/by/4.0/>).

Keywords: polycyclic aromatic hydrocarbons; sediments; Dachan Bay; Shenzhen city

1. Introduction

Polycyclic aromatic hydrocarbons (PAHs) are one of the most focused persistent organic pollutants with carcinogenicity, teratogenicity, and mutagenicity in the environments. Sixteen PAH monomers were listed as priority control pollutants by the United States Environmental Protection Agency (EPA) early in 1979. PAHs in the environment mainly originate from human activities, such as fossil fuels, biomass, and coal combustion [1]. Ma et al. (2020) [2] and Liu et al. (2012) [3] showed that PAHs pollution was closely related to the local social and economic development and energy consumption structure. Therefore, PAH pollution in environments are often studied to discuss the influence of human activities on the environment. Due to the hydrophobicity and migration of PAHs in the environment, PAHs in the atmosphere, water, and soil are finally settling in marine sediments, so the vertical profile of PAHs in core sediments could reveal the long-term impact of human activities on the environment [4–7].

Bay environments are one of the areas affected most by human activities while it is seriously threatened by pollutants from the surrounding areas [8]. High PAHs concentration has been detected in sediments from the bay in China, e.g., Bohai Bay (25 ng/g–280 ng/g) [9] and Quanzhou Bay (9 ng/g–108 ng/g) [10]. The concentrations

of PAHs in the core sediments of St. Lawrence Bay ranged from 93 ng/g to 172 ng/g before industrialization (1006–1822 CE) but increased to 1216 ng/g–1621 ng/g during industrialization (1937–1943 CE) [11].

Shenzhen is a special economic zone in China, and its average annual growth rate of GDP has reached 21.1% since 1978 (Shenzhen Statistical Yearbook, 2021). It is one of the fastest-growing cities in China. Dachan Bay (DCB) is located in the western region of Shenzhen, surrounded by industrial districts (Bao'an District and Nanshan District). Dachan Bay, with a port, has been the central area of marine economic development in western Shenzhen. DCB was originally a semi-circular open shallow bay. Due to the construction of DCB Port and the reclamation of seawalls at the mouth of the bay, the bay has become a relatively closed bay with a 1 km mouth, resulting in the weakening of hydrodynamic forces in the bay and serious sediment deposition [12]. Pollutants discharged from the surrounding areas accumulate in the bay, and the water quality of the coastal waters has long been inferior to the fourth category (Shenzhen Ecological Environment Status Bulletin, 2021); that is, the water quality is worse than the requirement of the general industrial water area and the recreational water area where the human body is not in direct contact. In recent years, the urban area and port area around DCB have developed rapidly, and environmental pollution has become one of the main problems restricting the sustainable development of DCB. Yang et al. (2020) research shows that the heavy metal content in the core sediments of DCB has increased due to human activities [13]. At present, there are few reported studies regarding PAHs in DCB. This study investigated the content, composition, distribution sources, and variation trend of PAHs in surface and core sediments of DCB to provide an understanding of the long-term impact of urban development and regional energy structure on the marine environment, further providing data for the control environmental policy of marine organic pollution.

2. Materials and Methods

2.1. Sample Collection

Thirteen surface sediment samples (Y1–Y10 in the sea, R1–R3 in the estuary) and a core sediment (S1) were collected in 2014 and 2016, respectively (Table 1 and Figure 1). The sampling depth of core sediments was 1.9 m, of which 0 m–1 m was separated by 5 cm, and the other was stratified by 10 cm. The sediment samples were freeze-dried, ground, sieved through 80 mesh, and stored in a dry environment in glass bottles.

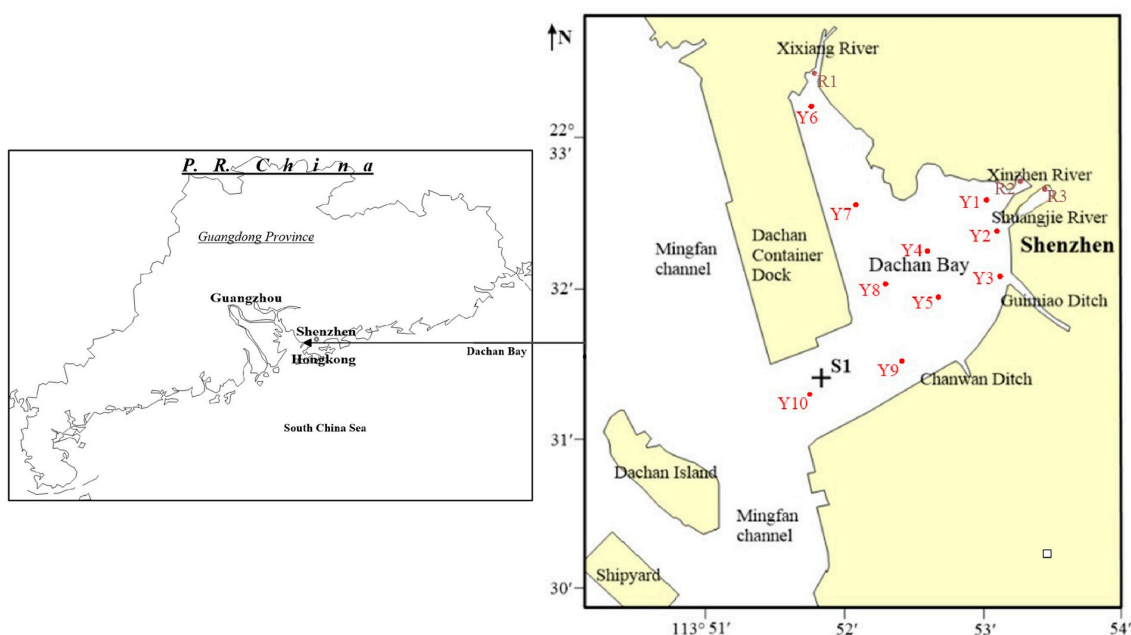


Figure 1. Map of the study area and sampling sites.

Table 1. Sampling ID and sampling location.

Sampling ID	Longitude	Latitude	Sampling ID	Longitude	Latitude
	E	N		E	N
Y1	113°52'56.64"	22°32'33.68"	Y8	113°52'18.29"	22°31'58.87"
Y2	113°53'3.62"	22°32'22.51"	Y9	113°52'26.01"	22°31'30.01"
Y3	113°53'5.11"	22°32'2.35"	Y10	113°51'39.68"	22°31'14.27"
Y4	113°52'34.96"	22°32'12.39"	R1	113°51'45.4"	22°33'30.0"
Y5	113°52'41.09"	22°31'49.09"	R2	113°53'08.6"	22°32'44.8"
Y6	113°51'43.85"	22°33'9.39"	R3	113°53'27.0"	22°32'40.1"
Y7	113°52'0.85"	22°32'35.22"	S1	113°51'48.27"	22°31'22.97"

2.2. Sample Pre-Treatment

Surface sediments were extracted by microwave extraction digestion instrument (MARS, CEM): 5 g samples were mixed with 8 g anhydrous sodium sulfate in an extraction tank, and the extraction solvent was 30 mL acetone/hexane (1:1, *v/v*) mixed reagent. Extraction conditions: the temperature was raised to 110 °C within 10 min, static extraction for 10 min, then cooled. The extract was poured out, and the extraction was repeated once. After the extraction liquid was combined, the sulfur was removed by a copper sheet, and the solvent was replaced by n-hexane. The solution was concentrated to 1 mL and purified by a 10 cm silica gel column, and eluted with 10 mL n-hexane and 70 mL dichloromethane/hexane (1:3, *v/v*), respectively. The latter was collected and concentrated at 0.5 mL.

The core sediment was extracted by the soxhlet extraction method. A total of 10 g of sample and 10 g of anhydrous sodium sulfate were mixed and loaded in a filter paper tube, 180 mL of dichloromethane was taken in a distillation bottle, and a certain amount of copper was added. The extract was concentrated to 3 mL, replaced twice with n-hexane, then concentrated to about 0.5 mL, transferred to the sample bottle, and diluted to 0.5 mL.

2.3. Analytical Method

PAHs were qualitatively and quantitatively analyzed by gas chromatography/mass spectrometry (TRACE GC ULTRA/TSQ QUANTUM XLS, Thermo SCIENTIFIC). The column was TR-1MS (30 m × 0.25 mm × 0.25 μm). The analysis conditions were as follows: the initial temperature of the column temperature box was 50 °C, increased to 200 °C at 5 °C/min, then increased to 290 °C at 8 °C/min, maintained for 3 min, and increased to 300 °C at 10 °C/min, maintained for 3 min. The inlet temperature and detector temperature were 280 °C and 300 °C, respectively. The carrier gas was helium, and argon was the collision gas. Selective Reaction Monitor scanning mode was used.

PAH standard products are Naphthalene (Nap), Acenaphthylene (Acy), Acenaphthene (Ace), Fluorene (Flu), Phenanthrene (Phe), Anthracene (Ant), Fluoranthene (Fla), Pyrene (Pyr), Benzo[a]anthracene (BaA), Chrysene(Chr), Benzo[b]fluoranthene (BbF), Benzo[k]fluoranthene (BkF), Benzo[a]pyrene (BaP), Indeno[1,2,3-cd]pyrene (IcdP), Dibenzo[a,h] anthracene (DahA), and Benzo[g,h,i]perylene (Bghip). The standard reagents for substitutes were Ace-D10 and Pyl-D12; the internal standards were Pentachloronitrobenzene (PNCB) and p-Terphenyl-D14.

2.4. Sediment Dating

Radioactive ²¹⁰Pb dating of the sample was performed with a 720008 eight-way alpha spectrometer (Canberra Company) at the Marine Institute of Oceanography, Ministry of Natural Resources. Using ²⁰⁹Po as the internal yield tracer, the radioactive activities of ²¹⁰Po produced by the decay of ²¹⁰Pb were determined, and thus, the radioactive activities of ²¹⁰Pb were calculated. The deposition rate and the chronology were calculated by the constant initial concentration (CIC) model [14–17]. The deposition rate calculated by the least squares method was about 1.09 cm/a.

2.5. QA/QC

Naphthalene is highly volatile and has a high background value in the air, which changes greatly and interferes with the analysis of other monomers, so it is not discussed here. We used the method blank, spike blank, matrix spike, parallel sample, and other methods for quality control. Acenaphthene-D10, Phenanthrene-D10, Chrysene-D12, and Perylene-D12 were used as recovery indicators of PAHs. The recovery rate was $73.4\% \pm 18.7\%$, $84.8\% \pm 16.5\%$, $76.8\% \pm 10.7\%$, and $69.1\% \pm 19.7\%$, respectively. The quantitative method was the internal standard method, and the quantitative results of PAHs were corrected by recovery and blank.

2.6. Statistical and Graphical Analysis

All statistical analyses (mean, standard deviation, minimum, maximum, Pearson's correlation matrix, and principal component analysis (PCA)) were performed using OriginPro 2022 SR1. Variability maps were created using the Surfer 15 software.

3. Results and Discussion

3.1. Content and Spatial Distribution of Σ_{15} PAH in Surface Sediments of DCB

In the surface sediments of DCB, 15 PAH compounds were detected, and their total concentrations (Σ_{15} PAH) were shown in Figure 2. The concentrations of Σ_{15} PAH ranged from 299 ng/g to 1474 ng/g, with an average of $734 \text{ ng/g} \pm 462 \text{ ng/g}$. The concentrations at Y2, Y6, and Y9 were the highest, which were 1173 ng/g, 1435 ng/g, and 1474 ng/g, respectively. Site Y8 and Y10 had the lowest concentrations of 341 ng/g and 299 ng/g, respectively. The concentrations of Σ_{15} PAH in Xixiang River (R1), Xinzhen River (R2), and Shuangjie River (R3) were 1032 ng/g, 2336 ng/g, and 1204 ng/g, respectively.

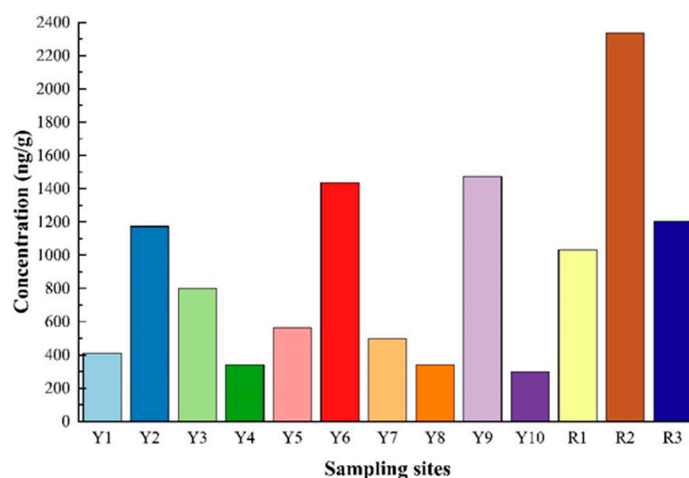


Figure 2. Concentrations of Σ_{15} PAH in surface sediments of DCB.

Compared with other bays and estuaries in China and abroad, the mean concentration of Σ_{15} PAH in sediments of DCB is higher than that of Yazhou Bay (32 ng/g) [18], Kaohsiung Port (352 ng/g) [19], Daya Bay (103 ng/g) [20], Yangtze Estuary Dam (146 ng/g) [21], Jiangsu Sheyang River (248 ng/g) [22], Pearl River Estuary Delta estuary location (291 ng/g) [23], and Tunisia Meliane River (77 ng/g) [24], and lower than that of Jiangsu Xinyanggang River (3209.46 ng/g) [22] and South Africa Algoa Bay (5230 ng/g) [25]. The comparison of results suggests that the current contamination levels of PAHs in DCB are moderate compared to other bays around the world and in China.

As seen in Figure 3, the concentrations of Σ_{15} PAH in DCB gradually decreased from the coastal to the central areas. The concentrations of Σ_{15} PAH in estuaries (R1, R2, and R3) were higher than those in adjacent sea areas, such as Y9 (Chanwan Ditch), Y6 (Xixiang River), Y2 (Guimiao Ditch), and Y3 (Shuangjie river). These rivers are the main urban rivers flowing into DCB and flowing through the populated and industrial districts. For

example, the Xixiang river flows through the Bao'an district with many industrial parks; the Shuangjie River flows through Tongle industrial area and Lishan operation area in Nanshan District and is close to the No.3 enclosure farm; Xinzhen River flows through many communities with wading enterprises, bazaars, and residential areas. Guimiao Ditch and Chanwan Ditch were seriously silted due to incomplete sewage interception, non-point source pollution, and insufficient estuary hydrodynamics. Therefore, vast living and industrial wastewater and gas are discharged into DCB.

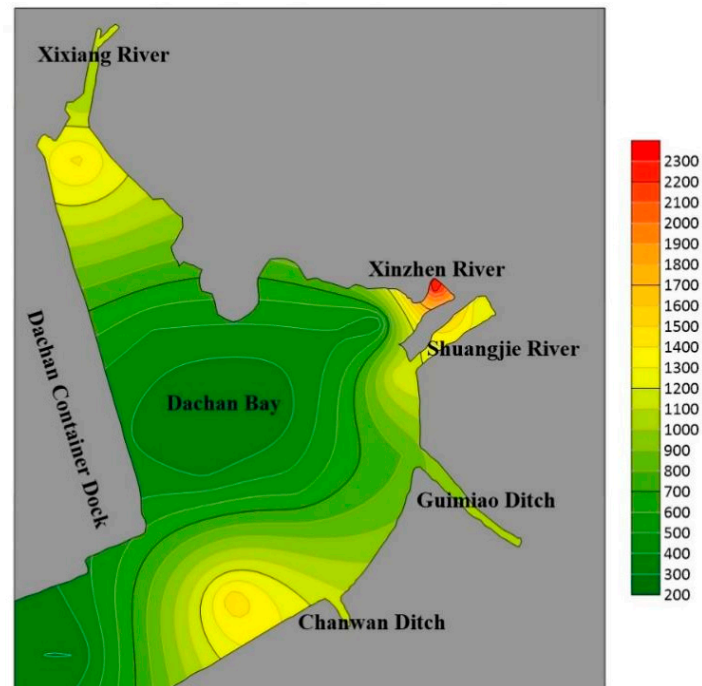


Figure 3. Spatial distribution of PAHs in surface sediments of DCB.

3.2. Content and Vertical Variation of Σ_{15} PAH in Core Sediments of DCB

The concentrations of Σ_{15} PAH in the core sediments of DCB ranged from 65 ng/g to 994 ng/g, with an average of 227 ng/g \pm 196 ng/g. The vertical variation is shown in Figure 4. The concentrations of Σ_{15} PAH varied greatly in the depth of 0 cm–60 cm (i.e., after 1950); their concentrations of Σ_{15} PAH ranged from 65 ng/g to 994 ng/g, with an average of 346 ng/g \pm 274 ng/g, and the relative standard deviation was 79%. The concentrations of Σ_{15} PAH below 60 cm depth ranged from 106 ng/g to 235 ng/g, with an average of 149 ng/g \pm 9 ng/g, and the relative standard deviation was 6.27%.

The vertical profile of Σ_{15} PAH in the core sediments of DCB is consistent with the urban development history of Shenzhen. Since 1949, the concentrations of Σ_{15} PAH in DCB have fluctuated greatly (Figure 4). The high concentration of Σ_{15} PAH in 1959 may be related to the “Great Leap Forward” movement. At that time, the construction of railways and steelmaking was prevalent in China, burning a lot of grass, wood, and coal [26]. The other high concentration of PAHs in 1991 was closely related to the rapid growth of population, industry, and energy consumption since the birth of Shenzhen Special Economic Zone. In the same period, Shenzhen issued the “Shenzhen Special Economic Zone Environmental Protection Regulations” in September 1994 to strengthen environmental supervision and remediation. This may be an important reason for the decrease in the concentrations of Σ_{15} PAH in DCB in the middle and late 1990s. The increase in energy consumption caused by private cars and industrial development may be the main reason for the high PAH concentration in 2002 (Shenzhen Statistical Yearbook, 2003).

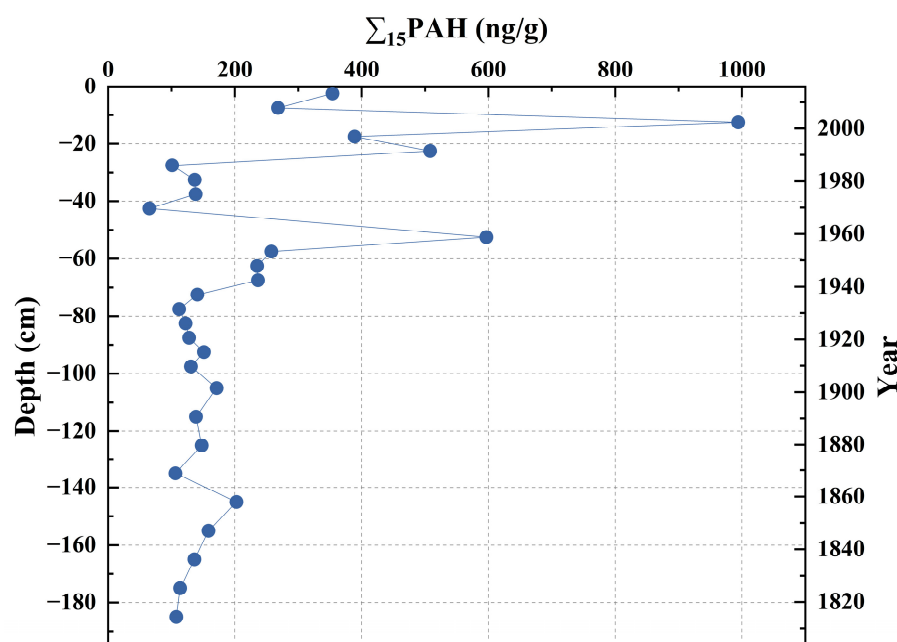


Figure 4. Vertical profile of the total PAHs in core sediments in DCB.

^{210}Pb dating has become a standard technique for the determination of recent (100–150 years) sedimentary geochronologies. In this study, ^{210}Pb dating was used to determine a core sediment at the mouth of Dachan Bay. The extrapolated chronologies below the ^{210}Pb dating horizon were estimated based on the measured average deposition rate. At the same time, the disturbance of the core sediment during sediment formation and the change in stress and strain during the collection of the core sediment may lead to the deviation of the dating results. Additionally, we also inferred the validity of the dating and such extrapolation by comparing the relative consistency of the overall PAHs change trend with the development history of Shenzhen. In our future study, the direct validity of the dating and extrapolation will be further conducted in the region. In addition, the data collected from only one core sediment at the mouth of the bay, which was susceptible to hydrodynamic and biodisturbance, may be insufficient to a certain degree. However, considering few studies on organic pollution in Dachan Bay, we still wish publish this paper, to provide a reference for relevant research and policy making, and also hope that readers view the data objectively. Additionally, in our future study, we will further adopt more reasonable sampling methods and dating techniques to investigate further the sedimentary feature in the region.

3.3. Composition Characteristics of PAHs in Sediments of DCB

Figure 5 shows the average concentrations of 15 PAH monomers in the surface sediments, estuarine surface sediments, and core sediments of DCB. In the surface sediments, BbF (120 ng/g) was the most abundant compound, followed by Pyr (114 ng/g), and Ace (3 ng/g) was the poorest. In the estuary sediments, Pyr (271 ng/g) was the most abundant compound, followed by Fla (270 ng/g), and Ace (5 ng/g) was the poorest. In the core sediments, Chr (47 ng/g) was the most abundant compound within the 0 cm–60 cm depth horizon, followed by Pyr (44 ng/g), and Ace was the poorest (1 ng/g). However, at the depth below 60 cm, BbF (22 ng/g) was the richest, followed by Phe (19 ng/g), and Ace (1 ng/g) was the poorest.

The 15 PAH monomers were divided into 3–6 ring PAHs according to ring size. As shown in Figure 6, PAHs in the surface sediments and the estuary were dominated by 4-ring, accounting for 36.42–54.22% and 49.00–54.53% of $\Sigma_{15}\text{PAH}$, respectively, followed by 5-ring, accounting for 22.47–34.14% and 19.13–21.52%, respectively. The results indicate that the PAHs are likely to be from combustion emissions of heavy oil, gasoline, and coal,

which is similar to Ji et al. (2022) and Almeida et al. (2018) [27,28]. These similarities can be explained by the busy shipping and industrial activities. PAHs in the core sediments exhibited similar composition characteristics, which can be illustrated by the changes in energy demand and structures in the history of the local economic development. This case was also found in Daya Bay (4- and 6-ring, 1891–2010) [29], the northern South China Sea offshore (5- and 6-ring, early Holocene) [30], and the northern Adriatic Sea (4-ring, 2003–2013) [31].

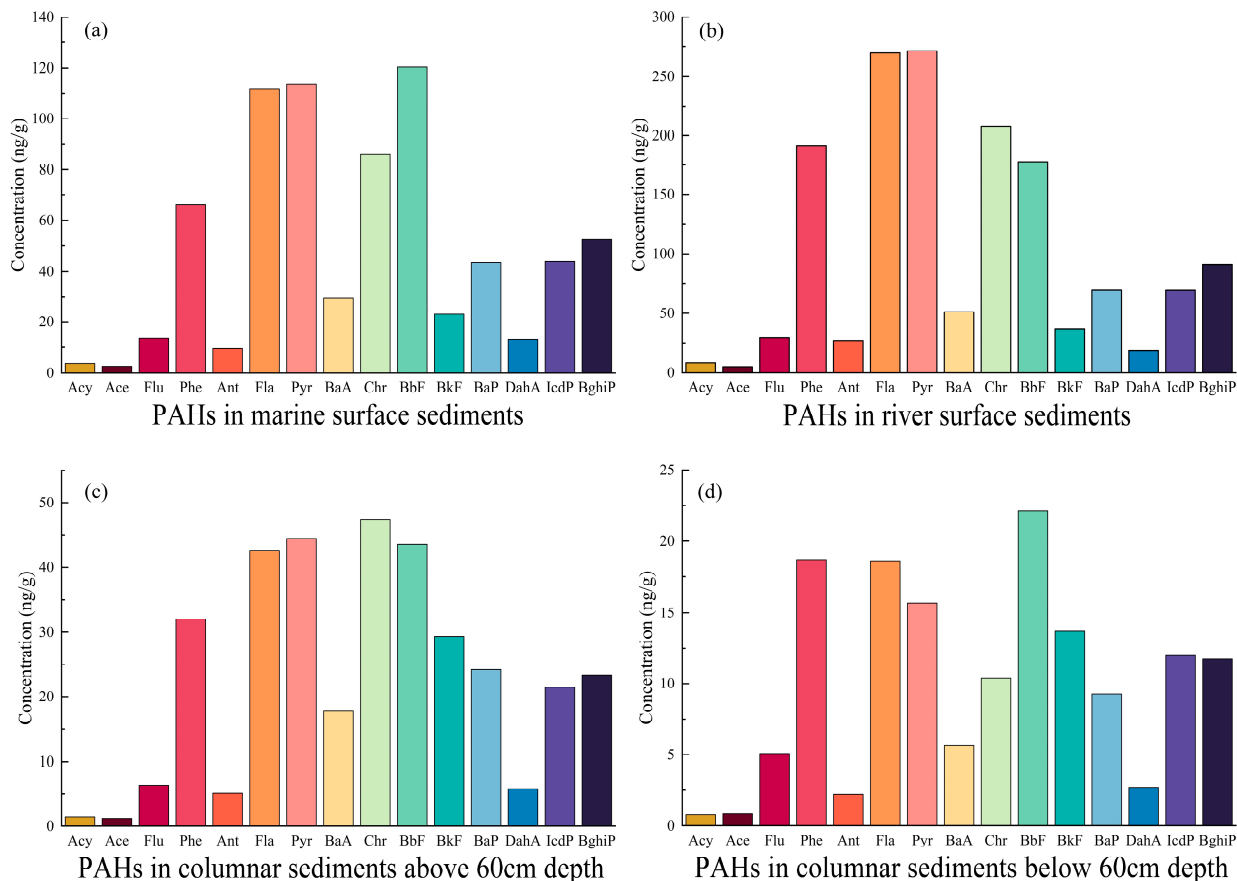


Figure 5. Concentrations of the 15 PAH monomers in surface sediments of DCB.

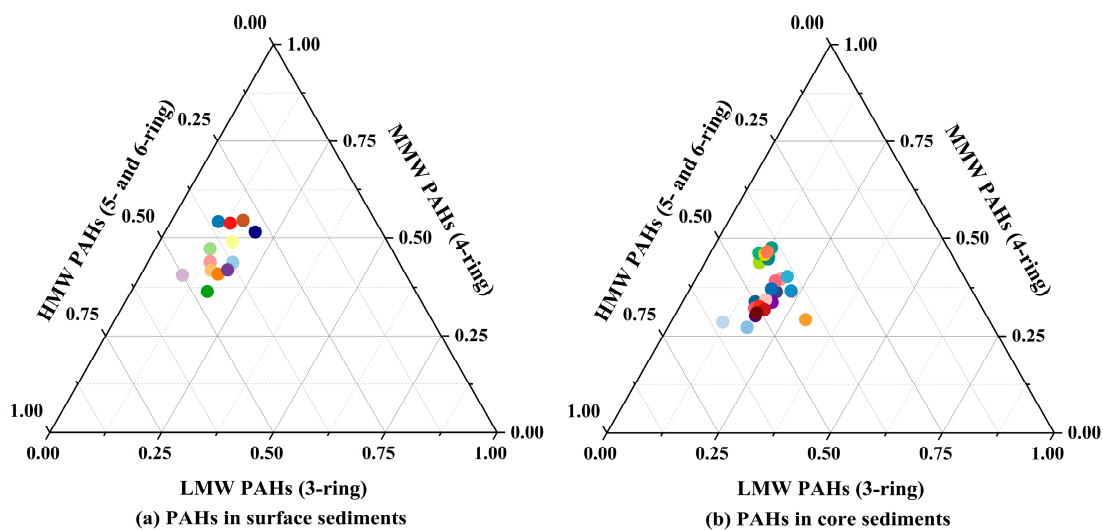


Figure 6. Triangular diagram of percentage concentrations for the 15 PAHs in sediments of DCB.

3.4. Source Analysis

According to molecular weight, PAHs are divided into low molecular weight PAHs (LMW PAHs, 2- and 3-ring), medium molecular weight PAHs (MMW PAHs, 4-ring) and high molecular weight PAHs (HMW PAHs, 5- and 6-ring). In general, LMW PAHs are from the spillage and leakage of petroleum, and HMW PAHs are from combustion sources. Therefore, the ratio of LMW/HMW is often used for source apportionment. It is considered that $LMW/HMW < 1$ implies the combustion source of PAHs, and the contrary is considered the petroleum source [32]. The LMW/HMW in the sediments of DCB was less than 1 (Figure 6), indicating that the PAHs in the sediments were mainly from combustion sources.

Some PAHs isomer ratios were also commonly used for inferring possible sources. The ratio of $Ant/(Ant + Phe) < 0.1$ usually implies a petrogenic source, whereas the ratio > 0.1 suggests a pyrogenic source. The ratio of $BaA/(BaA + Chr) < 0.2$ is attributed to petroleum, from 0.2 to 0.35 implies the mixed sources of petroleum and combustion, and > 0.35 indicates combustion. Ratios of $Fla/(Fla + Pyr) < 0.4$ and $IcdP/(IcdP + BghiP) < 0.2$ usually imply a petrogenic source, while $Fla/(Fla + Pyr)$ and $IcdP/(IcdP + BghiP) > 0.5$ indicate combustion of biomass (grass, wood, or coal combustion), and ratios of $Fla/(Fla + Pyr)$ from 0.4 to 0.5 and $IcdP/(IcdP + BghiP)$ from 0.2 to 0.5 suggest combustion of petroleum and byproducts [32–34].

3.4.1. Sources of PAHs in Surface Sediments

As shown in Figure 7, except for Y4, ratios of $Ant/(Ant + Phe)$ were higher than 0.1 for all other sampling sites. It indicated that the pollutants mainly originated from a pyrogenic source. The ratios of $IcdP/(IcdP + BghiP)$ for all samples were from 0.2 to 0.5, indicating a source of combustion of petroleum and byproducts in these 13 sites. This kind of source was confirmed by the ratios of $Fla/(Fla + Pyr)$ for most sampling sites (Y1–Y5, R1, and R2), which were from 0.4 to 0.5, while $Fla/(Fla + Pyr)$ were above 0.5 for other sites, revealing a source of combustion of biomass. The ratios of $BaA/(BaA + Chr)$ for most sampling sites (Y1, Y3–Y5, Y8, Y10, R1, and R3) were from 0.2 to 0.35, implying the mixed sources of petroleum and combustion; $BaA/(BaA + Chr)$ were below 0.2 in Y2, Y6, and R2, indicating petroleum; and $BaA/(BaA + Chr)$ were above 0.5 in Y7 and Y9, indicating combustion. The above isomer ratios of PAHs suggested that PAHs in DCB were mainly from the combustion of fossil fuels and biomass, associated with spillage of petroleum in several sampling sites. The results were consistent with the fact that there were frequent shipping activities in DCB and a large number of terrigenous inputs of pollutant. In 2013, large quantities of raw coal (about 4.03 million tons), crude oil (about 150,000 tons), gasoline (about 80,000 tons), kerosene (about 1500 tons), diesel (about 200,000 tons), fuel oil (5000 tons), and liquefied petroleum gas (about 20,000 tons) were consumed in industry. Moreover, the permanent year-end population was about 10.63 million, and the number of civil motor vehicles and transport vessels owned exceeded 2.6 million and 250, respectively, and freight traffic was about 300 million tons in Shenzhen (Shenzhen Statistical Yearbook, in 2014).

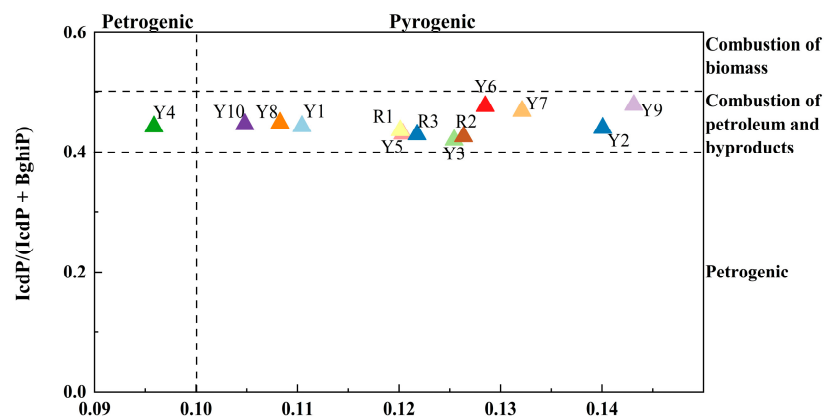


Figure 7. Cont.

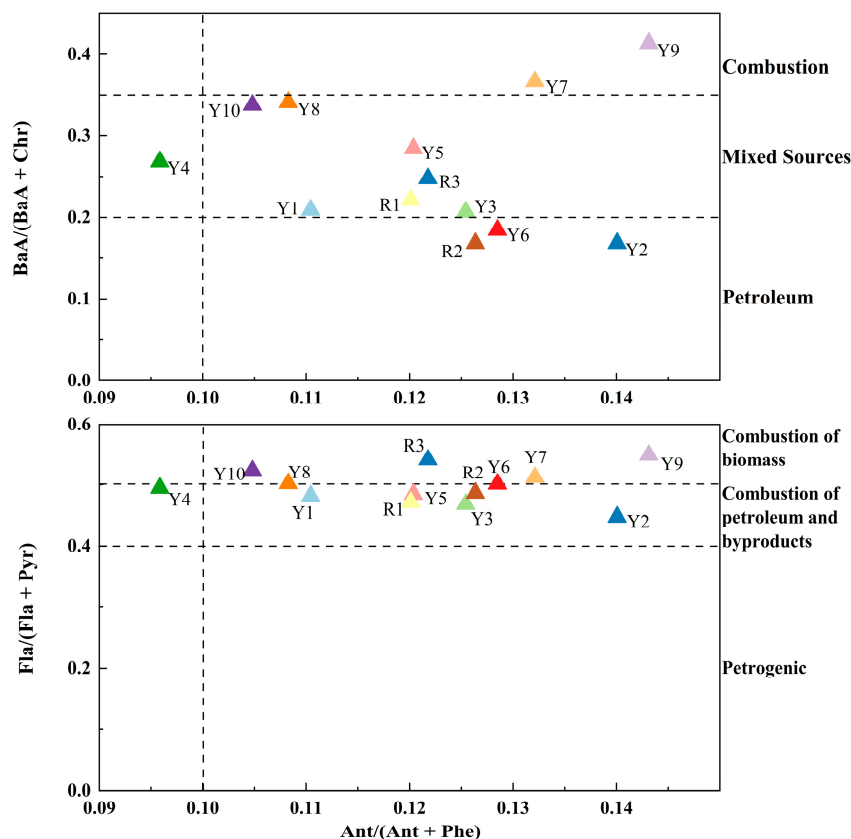


Figure 7. Diagnostic ratios of PAHs in surface sediments of DCB.

3.4.2. Sources of PAHs in Core Sediments

In Figure 8, the sources of PAHs in the core sediments of DCB are mainly mixed sources of oil, biomass, and coal combustion, occasionally accompanied by environmental pollution events such as oil leakage.

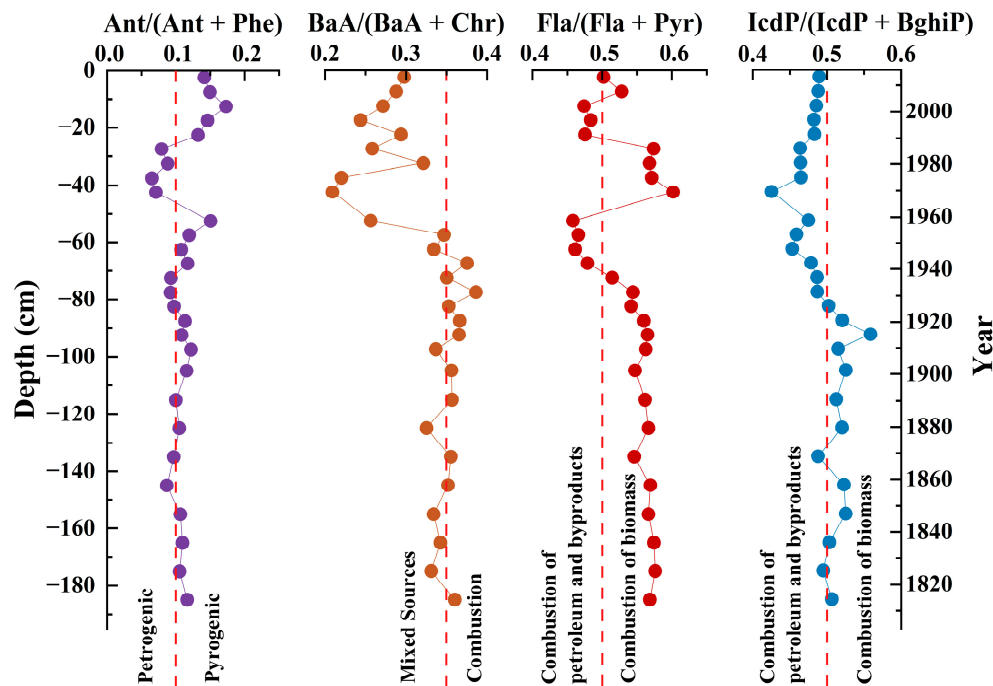


Figure 8. Diagnostic ratios for PAHs in core sediments of DCB.

In 60 cm–190 cm sediments (i.e., before 1950), ratios of Ant/(Ant + Phe), BaA/(BaA + Chr), Fla/(Fla + Pyr), and IcdP/(IcdP + BghiP) were generally near 0.1, near 0.35, greater than 0.5 and greater than 0.5, respectively, revealing that petrogenic sources and pyrogenic sources made an equal contribution, and indicating that the main pyrogenic source was the combustion of biomass. Specifically, the combustion of biomass was the main pyrogenic source before 1942, which was in line with the historical fact that Shenzhen was a small fishing village dependent on agriculture and fishing. After 1942, however, the combustion of petroleum and byproducts was the main pyrogenic source due to the intense war. Around 1942, Most areas of Guangdong province suffered from the Japanese bombing and occupation, Bao'an (the old name of Shenzhen) area was also affected [35]. Almost at the same time, the Hong Kong area fell, and a number of anti-Japanese armed forces gathered in Bao'an to fight [36,37].

In 0 cm–60 cm sediments (i.e., after 1950), the above isomer ratios of PAHs fluctuated greatly. Ratios of Ant/(Ant + Phe), BaA/(BaA + Chr), Fla/(Fla + Pyr), and IcdP/(IcdP + BghiP) were 0.27 ± 0.04 , 0.12 ± 0.04 , 0.52 ± 0.05 , and 0.47 ± 0.02 , respectively. The contribution of pyrogenic sources, especially combustion of petroleum and byproducts, was gradually highlighted. This was consistent with social and economic development and changes in the energy structure of Shenzhen, especially Bao'an District. In the early days of the founding of the People's Republic of China, in order to restore the domestic economy, the national crude oil production and the quantity demand for crude oil increased dramatically over several years. Around 1960, ratios of Ant/(Ant + Phe) increased significantly, implying the contribution from pyrogenic sources. At the same time, BaA/(BaA + Chr) decreased significantly. These results were closely related to popular activities, such as steelmaking, railway construction, and coal waste. From 1969 to 1986, Ant/(Ant + Phe) was less than 1, that was, the contribution of petrogenic PAHs was greater than that of pyrogenic PAHs, which reflected the economic regression caused by the "Great Leap Forward" and the "Cultural Revolution". The low concentration of Σ_{15} PAH between 1969 and 1986 (Figure 4) was evidence of this. Similar findings have been reported in other studies [2,38–40]. It was worth mentioning that the poor economic development represented by the low PAH concentration from 1978 to 1986 was not completely consistent with the known economic development history of the Shenzhen Special Economic Zone. In the 1990s, the ratio of Ant/(Ant + Phe) reflected the prominent contribution of pyrogenic sources, which was due to the consumption of the pyrogenic source associated with the rapid economic development of Shenzhen, which was dominated by industry and high-tech industries. However, due to the optimization of energy policy, the advocacy of sustainable development concepts and the operation of power plants, environmental pollution has been alleviated. However, around the 20th century, due to the popularity of automobiles and the development of trade, a large number of PAHs were still produced.

3.5. Correlation Analysis

In this study, oil and TOC in sediments were also investigated. Figure 9 shows the correlation between oil, TOC, and PAHs in surface sediments and core sediments.

Figure 9a showed that oil had a significant positive correlation with LMW PAHs, MMW PAHs, and Σ_{15} PAH ($r = 0.70$ – 0.90 , $p < 0.01$) but a weak positive correlation with HMW-PAHs ($r = 0.427$ – 0.477 , $p > 0.05$). The leakage of oil and the discharge of oily sewage from ships are important sources of PAHs [41,42], which are important contributors to LMW PAHs and MMW PAHs. The correlation was consistent with the characteristic ratios results. Oil in marine sediments mainly comes from the discharge of industrial and domestic oily wastewater from coastal cities, marine activities, and accidents of oil tankers. Oil pollution can have a variety of complex effects on the natural environment and can also be transferred and aggregated in the food chain due to biological magnification [43–45]. The correlation between oil and PAHs is consistent with the results of the above analysis of PAHs sources.

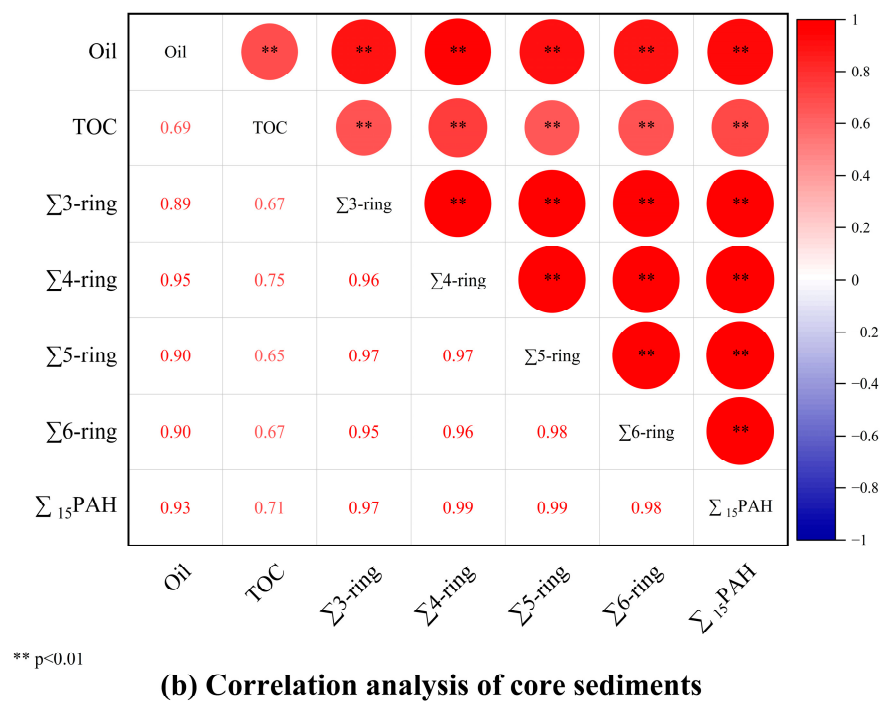
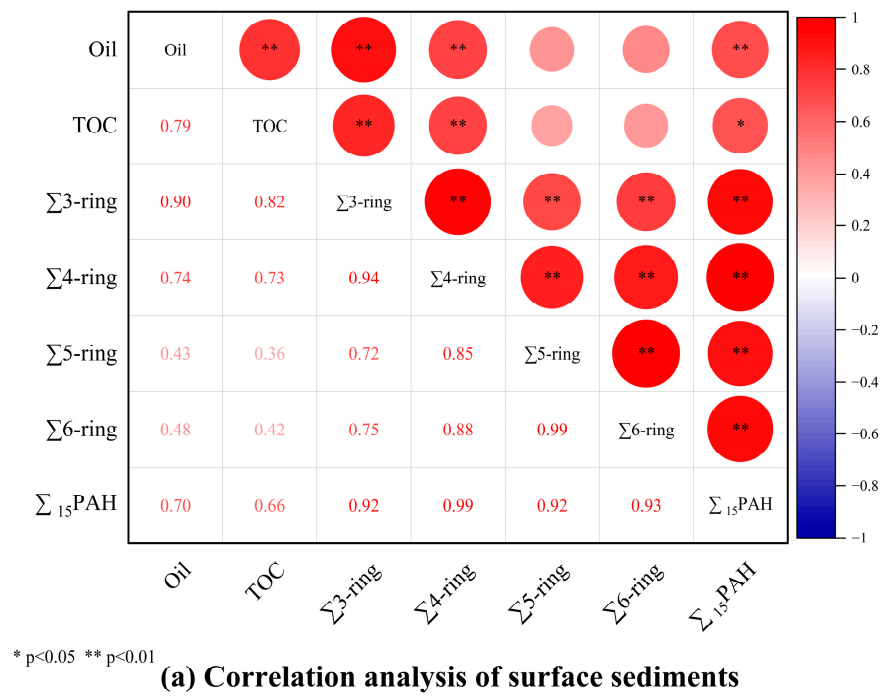


Figure 9. Correlation analysis of oil, TOC, PAHs of different ring numbers, and total PAHs in sediments of DCB.

The organic content in marine sediments has an important influence on the adsorption, migration, transformation, and degradation of pollutants in sediments. Total organic carbon (TOC) is one of the important indexes to reflect the content and quality of organic matter in marine sediments [46]. Figure 9a showed that TOC had a significant positive correlation with LMW PAHs and MMW PAHs ($r = 0.73\text{--}0.82$, $p < 0.01$) and Σ_{15} PAH ($r = 0.66$, $p < 0.05$), while TOC had a weak positive correlation with HMW PAHs ($r = 0.36\text{--}0.42$, $p > 0.05$). At present, the correlation between PAH content and TOC is still not conclusive. Chaber and Gworek (2020) identified that the correlation between PAH content and TOC content increased with the increase in PAHs molecular weight [47]. However, Abayi et al. (2021)

reported that the correlation between LMW PAHs and TOC is better [48]. In this study, the correlation between PAHs and TOC in surface sediments of DCB is more consistent with the report of the latter, that is, the correlation between middle and low cyclic number PAHs and TOC is better. This may be related to the octanol/water partition coefficient ($\log K_{ow}$) of PAHs. The $\log K_{ow}$ of LMW PAHs and MMW PAHs are smaller than that of HMW PAHs, which means that LMW PAHs and MMW PAHs easily dissolve in water, migrate with the flow and settle in sediments. Due to its high hydrophobicity and high lipophilicity, HMW PAHs are easily adsorbed by suspended particles in water. As a result, the time for HMW PAHs to enter the sedimentary facies is longer than that for LMW PAHs and MMW PAHs. In other words, there is a relative lag time [49].

Figure 9b showed that there was a significant positive correlation between oil, TOC, and PAHs with different ring numbers and total PAHs in core sediments compared with surface sediments, indicating that TOC and oil were important factors affecting the content and distribution of PAHs during the long-term deposition process.

4. Conclusions

The content and sedimentary record of PAHs in the surface and core sediments of DCB in Shenzhen city showed that urban development and human activities in Shenzhen have an important impact on the marine environment of DCB. In particular, the rapid economic development of Shenzhen after the reform and opening up has led to an increase in the content of PAHs in sediments. However, the content of PAHs in the sediments of DCB is at a medium level due to the protection and management of the marine environment of Shenzhen in recent years. Source analysis showed that PAHs in the sediments of DCB mainly came from a petrogenic source and combustion of biomass in the early stage. With the adjustment of production structure and the change of energy consumption structure, PAHs mainly came from the combustion of petroleum and byproducts. The correlation between TOC and PAHs shows that the TOC content in sediments affects the deposition of PAHs, and oil may be an important source of PAHs. This study shows that although the management of the marine environment has been strengthened, urban development and regional energy structure still have a great impact on the marine environment, and relevant departments still need to formulate and implement effective policies to control and improve the PAHs pollution in DCB.

Author Contributions: Conceptualization, W.H. and L.Z.; methodology, B.L. and L.Z.; software, W.H. and B.L.; validation, B.L. and L.Z.; writing—original draft preparation, W.H.; writing—review and editing, W.H., L.Z. and H.Z.; visualization, W.H.; project administration, J.Z. and H.Z.; funding acquisition, J.Z. and H.Z. All authors have read and agreed to the published version of the manuscript.

Funding: This research was funded by the National Natural Science Foundation of China, grant number 42076162.

Data Availability Statement: Data sharing is not applicable to this article.

Conflicts of Interest: The authors declare no conflict of interest.

References

1. Zhang, H.; Zhang, X.; Wang, Y.; Bai, P.; Hayakawa, K.; Zhang, L.; Tang, N. Characteristics and influencing factors of polycyclic aromatic hydrocarbons emitted from open burning and stove burning of biomass: A brief review. *Int. J. Environ. Res. Public Health* **2022**, *19*, 3944. [\[CrossRef\]](#)
2. Ma, X.; Wan, H.; Zhou, J.; Luo, D.; Huang, T.; Yang, H.; Huang, C. Sediment record of polycyclic aromatic hydrocarbons in Dianchi lake, southwest China: Influence of energy structure changes and economic development. *Chemosphere* **2020**, *248*, 126015. [\[CrossRef\]](#)
3. Liu, L.; Wang, J.; Wei, G.; Guan, Y.; Wong, C.; Zeng, E. Sediment records of polycyclic aromatic hydrocarbons (PAHs) in the continental shelf of China: Implications for evolving anthropogenic impacts. *Environ. Sci. Technol.* **2012**, *46*, 6497–6504. [\[CrossRef\]](#)
4. Chen, P.; Liang, J. Polycyclic aromatic hydrocarbons in green space soils in Shanghai: Source, distribution, and risk assessment. *J. Soils Sediments* **2021**, *21*, 967–977. [\[CrossRef\]](#)

5. Ya, M.; Wu, Y.; Wang, X.; Wei, H. Fine particles and pyrogenic carbon fractions regulate PAH partitioning and burial in a eutrophic shallow lake. *Environ. Pollut.* **2022**, *314*, 120211. [[CrossRef](#)]
6. Wu, G.; Qin, R.; Luo, W. Polycyclic aromatic hydrocarbons (PAHs) in the Bohai Sea: A review of their distribution, sources, and risks. *Integr. Environ. Assess. Manag.* **2022**, *18*, 1705–1721. [[CrossRef](#)]
7. Guo, F.; Gao, M.; Dong, J.; Sun, J.; Hou, G.; Liu, S.; Du, X.; Yang, S.; Liu, J.; Huang, Y. The first high resolution PAH record of industrialization over the past 200 years in Liaodong Bay, northeastern China. *Water Res.* **2022**, *224*, 119103. [[CrossRef](#)]
8. Sun, S.; Sun, X. *Theory and Practice of Gulf Ecosystem: A Case Study of Jiaozhou Bay*; Science Press: Beijing, China, 2015.
9. Wang, M.; Wang, C.; Hu, X.; Zhang, H.; He, S.; Lv, S. Distributions and sources of petroleum, aliphatic hydrocarbons and polycyclic aromatic hydrocarbons (PAHs) in surface sediments from Bohai Bay and its adjacent river, China. *Mar. Pollut. Bull.* **2015**, *90*, 88–94. [[CrossRef](#)]
10. Yang, D.; Qi, S.; Zhang, Y.; Xing, X.; Liu, H.; Qu, C.; Liu, J.; Li, F. Levels, sources and potential risks of polycyclic aromatic hydrocarbons (PAHs) in multimedia environment along the Jinjiang River mainstream to Quanzhou Bay, China. *Mar. Pollut. Bull.* **2013**, *76*, 298–306. [[CrossRef](#)]
11. Corminboeuf, A.; Montero-Serrano, J.-C.; St-Louis, R.; Dalpé, A.; Gélinas, Y. Pre-and post-industrial levels of polycyclic aromatic hydrocarbons in sediments from the Estuary and Gulf of St. Lawrence (eastern Canada). *Mar. Pollut. Bull.* **2022**, *174*, 113219. [[CrossRef](#)]
12. Sun, X.; Zhang, J.; Chen, C.; Liang, C.; Zhao, L. *Study on Environmental Capacity and Total Pollution Control Management in Shenzhen Sea Area of the Pearl River Estuary*; China Ocean Press: Beijing, China, 2017.
13. Yang, G.; Song, Z.; Sun, X.; Chen, C.; Ke, S.; Zhang, J. Heavy metals of sediment cores in Dachan Bay and their responses to human activities. *Mar. Pollut. Bull.* **2020**, *150*, 110764. [[CrossRef](#)] [[PubMed](#)]
14. Shukla, B.S.; Joshi, S.R. An evaluation of the CIC model of ²¹⁰Pb dating of sediments. *Environ. Geol. Water Sci.* **1989**, *14*, 73–76. [[CrossRef](#)]
15. Swarzenski, P.W. ²¹⁰Pb dating. In *Encyclopedia of Scientific Dating Methods*; Springer: Dordrecht, The Netherlands, 2014; pp. 1–11.
16. Zhang, J.; Mou, D.; Du, J.; Zhang, J. Study on comparison of excess ²¹⁰Pb chronology of several models. *Mar. Environ. Sci.* **2008**, *110*, 370–374.
17. Li, H.; Li, G.; Yang, F.; Gao, H.; Gong, Z.; Zhu, C.; Lian, J. Vertical Distribution Characteristics of Organochlorine Pesticides and Polychlorinated Biphenyls in Sediment Core from Lake Nansihu. *Environ. Sci.* **2007**, *28*, 1590–1594.
18. Han, B.; Li, Q.; Liu, A.; Gong, J.; Zheng, L. Polycyclic aromatic hydrocarbon (PAH) distribution in surface sediments from Yazhou Bay of Sanya, South China, and their source and risk assessment. *Mar. Pollut. Bull.* **2021**, *162*, 111800. [[CrossRef](#)]
19. Dong, C.; Chen, C.; Chen, C. Vertical profile, sources, and equivalent toxicity of polycyclic aromatic hydrocarbons in sediment cores from the river mouths of Kaohsiung Harbor, Taiwan. *Mar. Pollut. Bull.* **2014**, *85*, 665–671. [[CrossRef](#)]
20. Han, B.; Cui, D.; Liu, A.; Li, Q.; Zheng, L.; Research, P. Distribution, sources, and risk assessment of polycyclic aromatic hydrocarbons (PAHs) in surface sediments from Daya Bay, South China. *Environ. Sci. Pollut. Res.* **2021**, *28*, 25858–25865. [[CrossRef](#)]
21. Liu, X.; Chen, Z.; Wu, J.; Cui, Z.; Su, P. Sedimentary polycyclic aromatic hydrocarbons (PAHs) along the mouth bar of the Yangtze River Estuary: Source, distribution, and potential toxicity. *Mar. Pollut. Bull.* **2020**, *159*, 111494. [[CrossRef](#)]
22. Deng, X. *Yancheng Sources of PAHs in Sediment Distribution, the Sea and Its Response to Human Activities*. Master's Thesis, Information Engineering University, Nanjing, China, 2022.
23. Li, H.; Lai, Z.; Zeng, Y.; Gao, Y.; Yang, W.; Mai, Y.; Wang, C. Occurrence, source identification, and ecological risk assessment of polycyclic aromatic hydrocarbons in sediments of the Pearl River Delta, China. *Mar. Pollut. Bull.* **2021**, *170*, 112666. [[CrossRef](#)]
24. Khabouchi, I.; Khadhar, S.; Driouich Chaouachi, R.; Chekirbene, A.; Asia, L.; Doumenq, P. Study of organic pollution in superficial sediments of Meliane river catchment area: Aliphatic and polycyclic aromatic hydrocarbons. *Environ. Monit. Assess.* **2020**, *192*, 283. [[CrossRef](#)]
25. Adeniji, A.O.; Okoh, O.; Okoh, A.O. Distribution pattern and health risk assessment of polycyclic aromatic hydrocarbons in the water and sediment of Algoa Bay, South Africa. *Environ. Geochem. Health* **2019**, *41*, 1303–1320. [[CrossRef](#)]
26. Hou, W. *China's Economic Growth and Environmental Quality*; Science Press: Beijing, China, 2005.
27. Ji, B.; Liu, Y.; Wu, Y.; Gao, S.; Zeng, X.; Yu, Z. Distribution characteristics, sources and ecological risks of polycyclic aromatic hydrocarbons (PAHs) and oxygen-containing PAHs in sediments from the Yangtze Estuary and adjacent East China Sea. *Ecol. Environ. Sci.* **2022**, *31*, 1400–1408.
28. De Almeida, M.; do Nascimento, D.V.; de Oliveira Mafalda Jr, P.; Patire, V.F.; de Albergaria-Barbosa, A.C.R. Distribution and sources of polycyclic aromatic hydrocarbons (PAHs) in surface sediments of a Tropical Bay influenced by anthropogenic activities (Todos os Santos Bay, BA, Brazil). *Mar. Pollut. Bull.* **2018**, *137*, 399–407. [[CrossRef](#)]
29. Lu, Y.; Li, D.; Wang, X.; Cao, J.; Huang, S.; Zhou, P. Assessment and Implication of PAHs and Compound-Specific $\delta^{13}C$ Compositions in a Dated Marine Sediment Core from Daya Bay, China. *Int. J. Environ. Res. Public Health* **2022**, *19*, 4527. [[CrossRef](#)]
30. Gao, Y.; Xia, J.; Situ, J.; Tan, J.; Wang, S.; Wang, Y. Distribution and Source Identification of Polycyclic Aromatic Hydrocarbon of Core Sediments from Northern South China Sea. *J. Guangdong Ocean Univ.* **2021**, *41*, 111–116.
31. Bajt, O. Sedimentary Record of Polycyclic Aromatic Hydrocarbons in the Gulf of Trieste (Northern Adriatic Sea)—Distribution, Origin and Temporal Trends. *Front. Mar. Sci.* **2022**, *9*, 946618. [[CrossRef](#)]

32. Yunker, M.B.; Macdonald, R.W.; Vingarzan, R.; Mitchell, R.H.; Goyette, D.; Sylvestre, S. PAHs in the Fraser River basin: A critical appraisal of PAH ratios as indicators of PAH source and composition. *Org. Geochem.* **2002**, *33*, 489–515. [[CrossRef](#)]
33. Yuan, D.; Yang, D.; Wade, T.L.; Qian, Y. Status of persistent organic pollutants in the sediment from several estuaries in China. *Environ. Pollut.* **2001**, *114*, 101–111. [[CrossRef](#)]
34. Zhang, Z.; Hong, H.; Zhou, J.; Huang, J.; Yu, G. Fate and assessment of persistent organic pollutants in water and sediment from Minjiang River Estuary, Southeast China. *Chemosphere* **2003**, *52*, 1423–1430. [[CrossRef](#)]
35. Sui-jeung, C. *East River Column*; Hong Kong University Press: Hong Kong, China, 2009.
36. Ho, D.Y. Hong Kong, China: The border as palimpsest. *Made China J.* **2020**, *5*, 94–101. [[CrossRef](#)]
37. Zhu, S. Summary of the Preparation for Establishing the Anti-Japanese Armed Forces in Southern China in the Initial Stage of the Chinese War of Resistance against Japanese Aggression. *Mil. Hist.* **2016**, *213*, 35–40.
38. Xie, Z. Research on energy Policy of New China. Ph.D. Thesis, University of Science and Technology of China, Hefei, China, 2006.
39. Liu, G.; Zhang, G.; Li, X.; Li, J.; Peng, X.; Qi, S. Sedimentary record of polycyclic aromatic hydrocarbons in a sediment core from the Pearl River Estuary, South China. *Mar. Pollut. Bull.* **2005**, *51*, 912–921. [[CrossRef](#)]
40. Wu, H.; Wang, J.; Guo, J.; Hu, X.; Chen, J. Sedimentary records of polycyclic aromatic hydrocarbons from three enclosed lakes in China: Response to energy structure and economic development. *Environ. Pollut.* **2023**, *318*, 120929. [[CrossRef](#)]
41. Byrnes, T.A.; Dunn, R.J. Engineering. Boating-and shipping-related environmental impacts and example management measures: A review. *J. Mar. Sci. Eng.* **2020**, *8*, 908. [[CrossRef](#)]
42. Ytreberg, E.; Hansson, K.; Hermansson, A.L.; Parsmo, R.; Lagerström, M.; Jalkanen, J.-P.; Hassellöv, I.-M. Metal and PAH loads from ships and boats, relative other sources, in the Baltic Sea. *Mar. Pollut. Bull.* **2022**, *182*, 113904. [[CrossRef](#)]
43. Tsimplis, M. Marine Pollution from Shipping Activities. In *Maritime Law*; Informa Law from Routledge: London, UK, 2017; pp. 380–438.
44. Putatunda, S.; Bhattacharya, S.; Sen, D.; Bhattacharjee, C. A review on the application of different treatment processes for emulsified oily wastewater. *Int. J. Environ. Sci. Technol.* **2019**, *16*, 2525–2536. [[CrossRef](#)]
45. Zhang, B.; Matchinski, E.J.; Chen, B.; Ye, X.; Jing, L.; Lee, K. Marine Oil Spills—Oil Pollution, Sources and Effects. In *World Seas: An Environmental Evaluation*; Academic Press: Amsterdam, The Netherlands, 2019; pp. 391–406.
46. Avramidis, P.; Nikolaou, K.; Bekiari, V. Total organic carbon and total nitrogen in sediments and soils: A comparison of the wet oxidation–titration method with the combustion-infrared method. *Agric. Agric. Sci. Procedia* **2015**, *4*, 425–430. [[CrossRef](#)]
47. Chaber, P.; Gworek, B. Surface horizons of forest soils for the diagnosis of soil environment contamination and toxicity caused by polycyclic aromatic hydrocarbons (PAHs). *PLoS ONE* **2020**, *15*, e0231359. [[CrossRef](#)]
48. Abayi, J.; Gore, C.T.; Nagawa, C.; Bandowe, B.; Ssebugere, P. Polycyclic aromatic hydrocarbons in sediments and fish species from the White Nile, East Africa: Bioaccumulation potential, source apportionment, ecological and health risk assessment. *Environ. Pollut.* **2021**, *278*, 116855. [[CrossRef](#)]
49. Wang, W.; Qu, X.; Lin, D.; Yang, K. Octanol-water partition coefficient (logK_{ow}) dependent movement and time lagging of polycyclic aromatic hydrocarbons (PAHs) from emission sources to lake sediments: A case study of Taihu Lake, China. *Environ. Pollut.* **2021**, *288*, 117709. [[CrossRef](#)]

Disclaimer/Publisher’s Note: The statements, opinions and data contained in all publications are solely those of the individual author(s) and contributor(s) and not of MDPI and/or the editor(s). MDPI and/or the editor(s) disclaim responsibility for any injury to people or property resulting from any ideas, methods, instructions or products referred to in the content.